Progress of Theoretical Physics, Vol. 87, No. 5, May 1992

Statistics and Structures of Strong Turbulence in a Complex Ginzburg-Landau Equation

Hiroshi IWASAKI*) and Sadayoshi TOH

Department of Physics, Kyoto University, Kyoto 606-01

(Received December 16, 1991)

One-dimensional complex Ginzburg-Landau equation with a quintic nonlinearity (QCGL) is studied numerically to reveal the asymptotic property of its strong turbulence. In the inviscid limit, the QCGL equation tends to the nonlinear Schrödinger (NLS) equation which has a singular solution self-similarly blowing up in a finite time. The probability distribution function (PDF) of fluctuation amplitudes is found to have an algebraic tail with exponent close to -8. This power law is described as the multiplication of the PDF of the amplitude of a singular solution of the NLS equation and that of maximum heights of bursts. The former is shown to have a -7 power law in terms of the scaling property of the NLS singular solution. The latter is found to have a -1 power law by numerical simulation.

§ 1. Introduction

Significant deviations from Gaussian statistics make it difficult to understand the property of the fully developed turbulence. Non-Gaussianity observed in the probability distribution functions (PDFs) of the velocity gradients plays a fundamental role in the energy transfer. The nonzero skewness of the longitudinal velocity gradients induces the energy transfer toward small scales. The strong intermittency in the energy dissipation is reflected in the large flatness of the velocity gradients.[1)~3)]

Recently several authors have discussed the structures of PDFs.[4)~6)] She et al.[4)] showed by a Fourier-space band-filtering method that the flatness factors not only of the velocity derivatives but of the velocity fields are large when wave numbers involved are in the dissipation range. It is noteworthy that the PDFs of velocity gradients reconstructed with the Fourier modes in inertial range are close to Gaussian. These results suggest the existence of small-scale coherent structures, e.g., strong bursts in energy dissipation. The structures may be related to the complex-space singularities of the Navier-Stokes (NS) equations; in the inviscid limit, these singularities may appear in real-space in a finite time. Therefore it is plausible that the tail structures of the PDFs may be accounted for in terms of those coherent structures in the limit of high Reynolds number.

Introducing a mapping closure model based on this idea, Kraichnan and She [5),6)] tried to reproduce non-Gaussian PDF of the transverse velocity gradients obtained by direct numerical simulations at moderate Reynolds numbers. However, the characteristics of coherent structures are not clarified in their heuristic model. Anyway singularities of the Euler equations including their existence have not been explained thoroughly yet in spite of accumulation of researches.[7)~9)]

Our computational facilities are not powerful enough to simulate the NS equations at sufficiently high Reynolds numbers at which singularities may be visible if

*) Present address: Faculty of Education, Kanazawa University, Kanazawa 920.

they exist. In this paper, we study one-dimensional complex Ginzburg-Landau equation with a quintic nonlinearity (QCGL) to examine the relation between the singularity and the asymptotic tail structure of PDF. The QCGL equation has much simpler dynamics than the NS equations and shows some essential characteristics similar to those of the NS equations. In the non-dissipative or inviscid limit, the QCGL equation tends to a nonlinear Schrödinger (NLS) type equation which has singular solutions blowing up in a finite time.[10] As the dissipative effects become weak, the QCGL equation shows strongly chaotic and intermittent behavior due to bursting events localized in both space and time. These features are reminiscent of those of the NS equations. The fundamental features of these equations and their solutions are described together with the numerical methods in § 2. The PDFs of amplitudes increase deviation from Gaussian distribution with the decrease of the dissipative effects, and approach asymptotic forms in the inviscid limit.[11] These numerical results are shown in § 3. In § 4, the asymptotic tail structures of the PDFs are explained in terms of the singular solutions of the one-dimensional nonlinear Schrödinger equation involving a quintic nonlinearity (QNLS). Finally, § 5 is devoted to concluding remarks.

§ 2. Fundamentals

We consider the one-dimensional complex Ginzburg-Landau equation with a quintic nonlinearity (QCGL)

$$\frac{\partial\psi}{\partial t}=\frac{R}{\nu}\psi+\left(\frac{1}{\nu}+i\right)\frac{\partial^2\psi}{\partial x^2}+\left(-\frac{1}{\nu}+i\right)|\psi|^4\psi\,, \tag{1}$$

in a periodic interval $[0, 1]$, where variable $\psi(x, t)$ is a complex function of space x and time t, and R and ν are real positive parameters. Using these parameters, we introduce the characteristic time, length and height by ν/R, $R^{-1/2}$ and $R^{1/4}$, respectively.

If $\nu>1$, the system is modulationally unstable and has a chaotic behavior. When ν is relatively small, the system may be chaotic with a few degrees of freedom. The behavior of the solution becomes more complicated with increasing ν.[12]

In the limit of large ν, the QCGL equation approaches the QNLS equation,

$$\frac{\partial\psi}{\partial t}=i\frac{\partial^2\psi}{\partial x^2}+i|\psi|^4\psi\,, \tag{2}$$

which is known to have a singular solution blowing up at a finite time.[10),13)~17)] It has been shown[13)] that when the degree of nonlinear term $(2\sigma+1)$ and the spatial dimension d satisfy the relation $\sigma d\geq 2$, the NLS equation generally has a singular solution. In the one-dimensional case, the quintic nonlinearity $|\psi|^4\psi$ is the least power with which the system has a singular solution.

Equation (2) has a special solution $\psi(x, t)=e^{it/3}S(x)$, where amplitude $S(x)$ is governed by $d^2S/dx^2-(1/3)S+S^5=0$, which admits a localized solution

$$S(x)=\mathrm{sech}^{1/2}\left(\frac{2x}{\sqrt{3}}\right), \tag{3}$$

having the maximum value of unity at $x=0$. Furthermore, Eq. (2) has the following scaling property. If $\psi(x, t)$ is a solution, so is $\lambda^{-1/2}\psi(\lambda^{-1}x, \lambda^{-2}t)$, where λ is an arbitrary positive constant.

It is expected that a singular solution of Eq. (2) can be described by S which is scaled by a time-dependent factor $\lambda(t)$ decreasing to zero at the critical time, i.e., $\psi(x, t)\sim\lambda^{-1/2}(t)S(\lambda^{-1}(t)x)$. With this conjecture, many researchers[13)~15)] tried to determine this factor for the singular solutions of the NLS equation in the 1-D and 2-D cases, but their results did not agree with numerical results. Recently, a singular solution of the 2-D NLS equation has been studied by LeMesurier et al.[16),17)] Their result was found to agree well with that of numerical simulations.

By a straightforward application of their analytical method, Eq. (2) is found to have a singular solution, which blows up at a critical time t^*, of the form:

$$\psi(x, t)=L^{-1/2}\exp\left(i\frac{\tau}{3}-ia\frac{\xi^2}{4}\right)V(\xi, \tau), \tag{4}$$

where

$$L(t)\sim\left(\frac{t^*-t}{\ln\ln\left(\frac{1}{t^*-t}\right)}\right)^{1/2}, \xi=L^{-1}x, \tau=\int_0^t L^{-2}(s)ds, a=-L\frac{dL}{dt}. \tag{5}$$

The functional form of $V(\xi, \tau)$ near the origin is very close to that of a special solution $S(\xi)$. At large distance, on the other hand, $V(\xi, \tau)$ decreases only algebraically while $S(\xi)$ decreases exponentially. The region where V coincides with S expands slowly as t approaches the critical time, and they become completely identical with each other at the critical time.

The QCGL equation (1) may have a solution which behaves in a way similar to the above singular solution, though the dissipative effects suppress a blow-up. The system is disturbed by remnant and modulationally unstable modes.[11)] Bartuccelli et al.[12)] also predicted that the QCGL equation shows strongly chaotic and intermittent behavior, called *strong turbulence,* for sufficiently large R and ν.

We study this "turbulent" state by solving Eq. (1) numerically in terms of split-step time integration scheme[18)] with 1/3 de-aliased pseudo-spectral method. As will be shown in the next section, the solution sometimes takes extremely large amplitudes. The mesh size and the time step are optimized automatically so that the steep structure may be well resolved. When the higher wave number components are excited strongly, the mesh size is halved and the time step is quartered to avoid numerical instability. During the simulation the number of collocation points is changed between 2^{11} and 2^{17}. We set $R=10{,}000$ and $\nu=500$, which are sufficiently large for Eq. (1) to show the asymptotic behavior.[11)] When we rescale Eq. (1) as $\psi(x, t)\to R^{1/4}\psi(R^{1/2}x, Rt)$ to eliminate R from the equation, the system size becomes $R^{1/2}$ and the factors of non-conservative terms turn $1/\nu$. Thus 10^4 is sufficiently large to

examine the behavior of this system for the large system size. In this sense, this system for large ν may behave in a way similar to the QNLS equation even though ν is much smaller than R.

§ 3. Numerical results

In order to see the global spatio-temporal structure of solution $\psi(x, t)$, we plot in Fig. 1 the absolute value $|\psi(x, t)|$ for the whole spatial domain. The profile is shifted up in proportion to time. The variation of $|\psi(x, t)|$ in space and time is very complicated. The spatio-temporally localized structure, "burst", can be seen at $t=1.6077576$, $x=0.42$ and $t=1.6099750$, $x=0.15$. The relatively small amplitude waves with high wave numbers arise in the whole domain only for a short while after a burst appears.

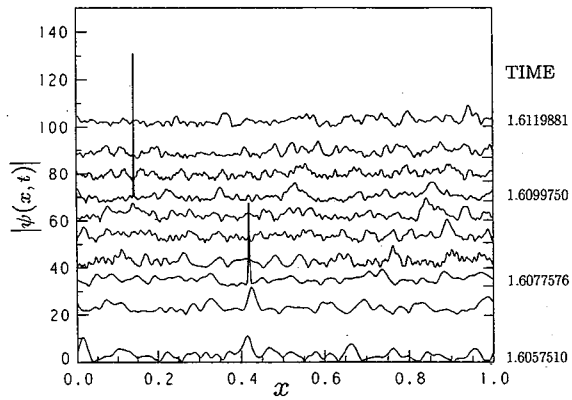

Fig. 1. Time evolutions of $|\psi(x, t)|$ for $\nu=500$ in the whole spatial domain. The right ordinates show time and each scale indicates the time of corresponding profile.

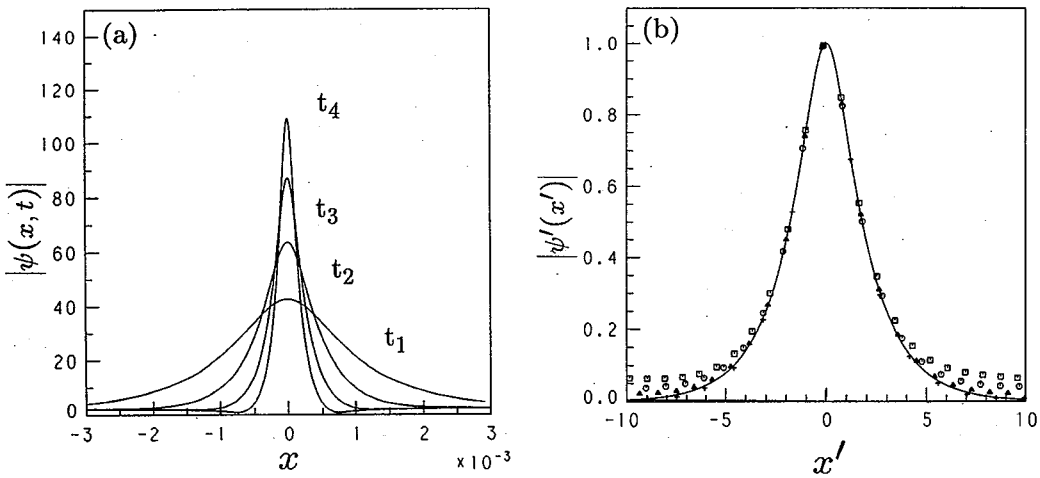

Fig. 2. (a) Enlarged plots of a burst in Fig. 1 at $t_1=1.6099742$, $t_2=1.6099750$, $t_3=1.6099752$ and $t_4=1.60997525$. The time step during this period is order of 10^{-9}. (b)Scaled profiles $|\psi'(x')|=\lambda^{1/2}|\psi(\lambda x')|$ where $\lambda=(\sup_x|\psi(x)|)^{-2}$ at $t_1(\square)$, $t_2(\circ)$, $t_3(\triangle)$ and $t_4(+)$. The signs are plotted every four mesh. The solid line represents $S(x')=\mathrm{sech}^{1/2}(2x'/\sqrt{3})$.

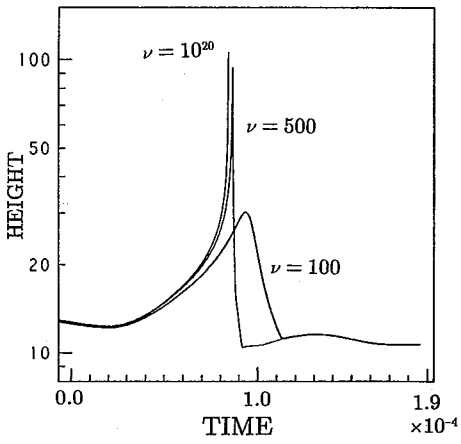

Fig. 3. Time-evolutions of the peak value of a burst for $\nu=100$, $\nu=500$ and $\nu=10^{20}$. The time origin has been redefined for convenience.

3.1. *Local structure of a single burst*

In Fig. 2(a), we enlarge a particular burst in Fig. 1. The shape of the burst is almost symmetric and its width is narrower as the height is larger. In Fig. 2(b) we normalize the shape using the scaling property of the QNLS equation at each time step so that the height is unity. The solid line is a special solution $S(x')=\mathrm{sech}^{1/2}(2x'/\sqrt{3})$, where x' is a scaled variable. The scaled shape is close to S near the origin. This fact indicates that the burst developes self-similarly like the singular solution of the NLS equation.

The time-evolutions of the peak value of the burst are shown in Fig. 3. For $\nu=500$, it first increases algebraically. After reaching a finite height it stops increasing and decays rapidly, because the dissipation terms, $\partial\psi/\partial x$ and $|\psi^4|\psi$, then become dominant. The curves for $\nu=100$ and $\nu=10^{20}$, the latter being regarded as the QNLS case, were calculated using the same data for $\nu=500$ as the initial condition. Note that with increasing ν, the maximum of the peak value increases and the time attaining the maximum approaches the critical time of the QNLS singular solution. It is remarkable that the time-evolution of the peak value of the burst for $\nu=500$ is very close to that of the singular solution of the QNLS equation.

In order to study spatio-temporal structures of this blow-up solution ($\nu=10^{20}$), we plot in Fig. 4(a) the shapes of the absolute value, $|\psi(x, t)|$, at several instants. As the peak value of $|\psi(x, t)|$ becomes larger, the width gets narrower. The figure suggests that this is the self-similar blow-up solution mentioned in the preceding section. This self-similarity implies that there is a scaling function $L(t)$ such that the solution ψ is described by a function V as $\psi(x)=L^{-1/2}V(L^{-1}x)$ at each time. Next we examine the shape of V and time dependent scaling factor $L(t)$.

For convenience the scaling function $L(t)$ is chosen as $L(t)=(\sup_x|\psi(x, t)|)^{-2}$ so that the rescaled function $V(L^{-1}x)=L^{1/2}\psi(x)$ has the maximum value of unity. The rescaled functions $|V(\xi)|$ at several instants are plotted in Fig. 4(b). The parameter ξ is shifted so that $|V|$ has the maximum at $\xi=0$. The solid line represents the special solution S. The shape of $|V|$ is almost identical to S except for the tail part. We note that the evolution of the burst in Fig. 2 is almost similar to that of the QNLS solution.

Furthermore, to investigate the scaling function, we show in Fig. 4(c) L against t^*-t in a logarithmic scale. The solid lines represent $L_0(t)=(t^*-t)^{1/2}$ and $L_1(t)=(t^*-t)^{1/2}(\ln\ln(1/(t^*-t)))^{-1}$. The factor L is well fitted by L_1 as t tends to t^*. However, it is also well approximated by L_0 especially near t^*. Note that the logarithmic correction in L_1, $(\ln\ln(1/(t^*-t)))^{-1}$, is slightly different from the theoreti-

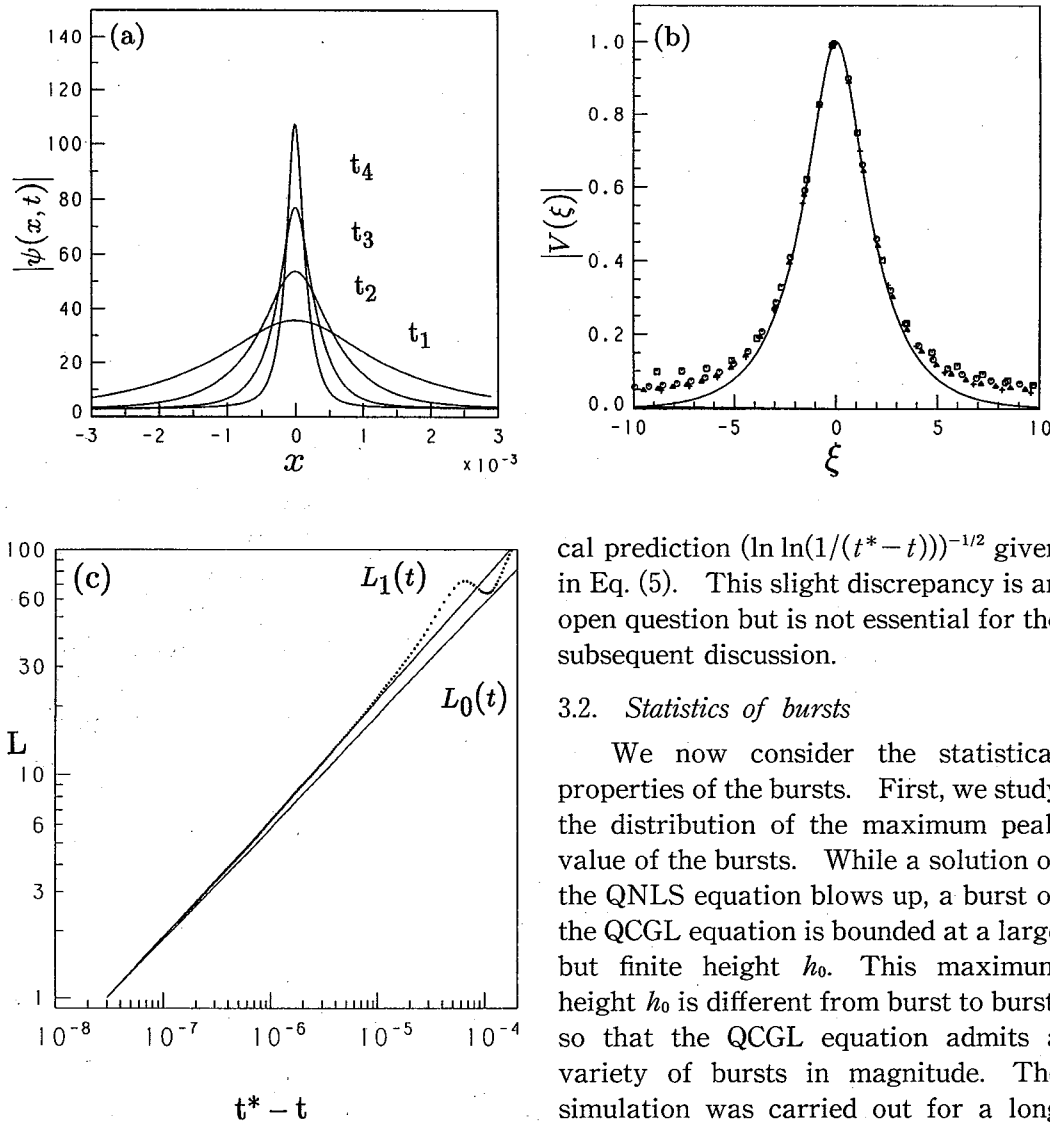

Fig. 4. (a) Enlarged plots of $|\psi|$ for $\nu=10^{20}$ at $t_1=1.6099720$, $t_2=1.6099734$, $t_3=1.6099737$ and $t_4=1.60997375$. The time step during this period is order of 10^{-9}. (b) Scaled profiles $|V(\xi)|$ at $t_1(\square)$, $t_2(\circ)$, $t_3(\triangle)$ and $t_4(+)$. The signs are plotted every four mesh. The solid line represents $S(\xi)$. (c) The scaling factor $L(t)$ plotted in comparison with $L_0(t)=(t^*-t)^{1/2}$ and $L_1(t)=(t^*-t)^{1/2}/\ln\ln(1/(t^*-t))$.

cal prediction $(\ln\ln(1/(t^*-t)))^{-1/2}$ given in Eq. (5). This slight discrepancy is an open question but is not essential for the subsequent discussion.

3.2. *Statistics of bursts*

We now consider the statistical properties of the bursts. First, we study the distribution of the maximum peak value of the bursts. While a solution of the QNLS equation blows up, a burst of the QCGL equation is bounded at a large but finite height h_0. This maximum height h_0 is different from burst to burst, so that the QCGL equation admits a variety of bursts in magnitude. The simulation was carried out for a long time enough to include more than 1,000 bursts for $\nu=500$.

In Fig. 5, we plot $G(h)$ the probability of such bursts that have maximum heights greater than h. Although $G(h)$ decreases rapidly at the small height around the characteristic height ($R^{1/4}=10$), there is a -1 power law range followed by a faster decay. By comparing $G(h)$ for other parameters ($\nu=100$, 200, 300, 400), we can see that the power law range increases with ν.

To characterize the intermittent property of the system, it is convenient to study the structure of the PDFs. Figure 6 shows the PDF of the real and imaginary parts

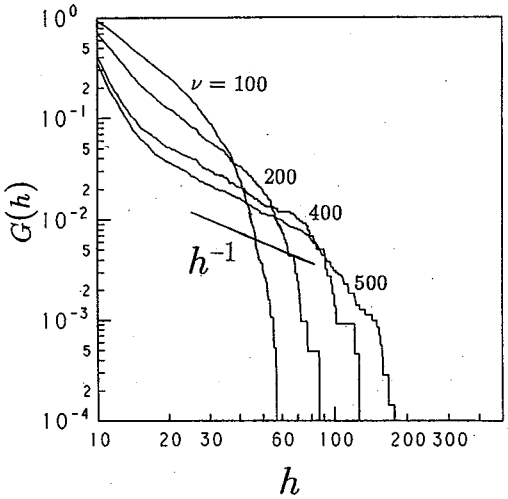

Fig. 5. The PDF $G(h)$ for ν=100, 200, 400, 500.

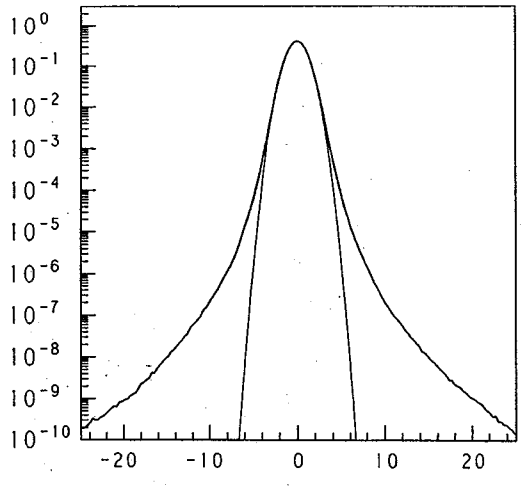

Fig. 6. The PDF of the real and the imaginary part of ψ. Gaussian distribution is plotted for comparison.

of the QCGL solution, Re($\psi(x, t)$) and Im ($\psi(x, t)$), which is normalized so that the standard deviation is equal to unity. (Since Eq. (1) is isotropic for the argument of ψ, the real and imaginary parts obey the same distribution.) The shape of the PDF around the central part is nearly Gaussian which is contributed from small amplitude waves. In contrast, at large amplitude it is significantly non-Gaussian with an algebraic tail, which reflects large bursts. This suggests that non-Gaussianity may not be observed strongly in lower-order moments. Indeed, the skewness factor is zero within numerical errors and the flatness factor is 3.4 (as compared to the Gaussian value of 3).

Now we consider the following PDF of the absolute value $|\psi(x, t)|$ defined by

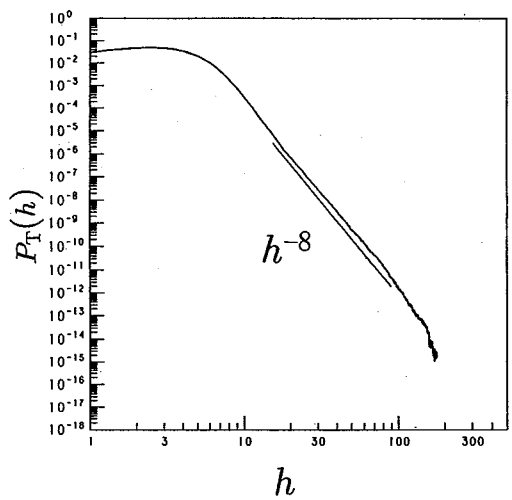

Fig. 7. The PDF $P_T(h)$.

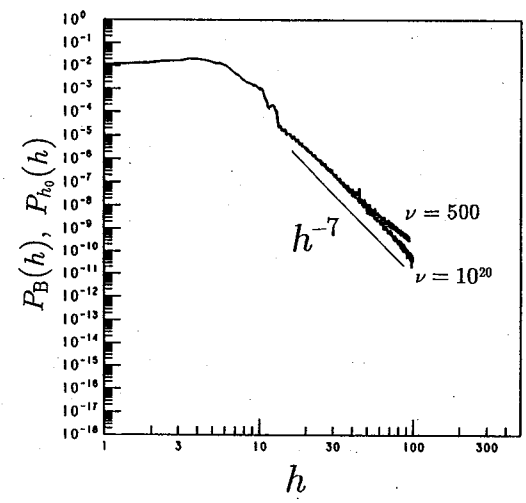

Fig. 8. The PDFs $P_B(h)$ (ν=500) and $P_{h_0}(h)$ (ν=10^{20}) for h_0=100.

$$P(h)=\frac{\iint dtdx\delta(|\psi(x,t)|-h)}{\iint dtdx}. \tag{6}$$

Three particular PDFs are important in the following discussion. The first PDF, $P_T(h)$, is obtained from the QCGL solution, integrated over the whole spatio-temporal domain. The second one, $P_B(h)$, is obtained from a single burst, whose integral is over the whole spatial domain and its lifetime. Finally, $P_{h_0}(h)$ is obtained from the blow-up solution of the QNLS equation, integrated over the whole spatial domain from its birth to the time of the maximum height h_0.

In Fig. 7, we plot $P_T(h)$ which has an algebraic tail with an exponent -8. In Fig. 8, $P_{h_0}(h_0=100)$ and $P_B(h)$ are shown. They have almost the same algebraic tail with an exponent -7. The reason why P_B decreases slower than P_{h_0} for large h is that the dissipation effects suppress the growth of bursts near the maximum amplitude. The difference in the exponent between P_T and P_B should be explained by the statistical distribution of the bursts.

In the next section, we will first explain the power law -7 for P_{h_0} or P_B by the scaling property of the QNLS singular solution and then try to reconstruct the power law -8 for $P_T(h)$ in terms of $P_B(h)$ and $G(h)$.

§ 4. Explanation of the power law of PDF

In the preceding section, we see that $P_T(h)$ has the power law -8. This power law should be attributed to the statistics of bursts. Since bursts with very large amplitude behave in a way similar to the singular solution, the power law of P_B may be explained in terms of the scaling law of the singular solution of the QNLS equation.

As the first step, we estimate $P_\infty(h)$, i.e., $P_{h_0=\infty}(h)$, defined as

$$P_\infty(h)=\frac{\int^{t^*}\int dtdx\delta(h-|\psi(x,t)|)}{\int^{t^*}\int dtdx}, \tag{7}$$

where ψ is a singular solution of the QNLS equation and t^* is its blow-up time.

To estimate Eq. (7), we use singular solution (4). Near the critical time t^*, the logarithmic dependence of L on time (t^*-t) can be neglected and V can be approximated by S. Hence the solution can be approximated as

$$|\psi(x,t)|=\lambda^{-1/2}S(\xi),\quad \xi=\lambda^{-1}x,\quad \lambda=(t^*-t)^{1/2}. \tag{8}$$

Using new variables ξ and λ, we find

$$P_\infty(h)\propto\int_\infty^0\frac{d\lambda}{\frac{d\lambda}{dt}}\int_{-\infty}^{\infty}\lambda d\xi\delta(h-\lambda^{-1/2}S(\xi))$$

$$=4\int_{-\infty}^{\infty}d\xi\int_0^\infty d\lambda\frac{\lambda^{7/2}}{S(\xi)}\delta\left(\lambda-\left(\frac{S(\xi)}{h}\right)^2\right)$$

$$=4h^{-7}\int_{-\infty}^{\infty}d\xi S(\xi)^6 \quad (=\sqrt{3}\pi h^{-7})\,. \tag{9}$$

Thus we get $P_\infty(h)\propto h^{-7}$. This power law agrees well with the numerical result in Fig. 8.

In order to explain the -8 exponent of $P_T(h)$ for the QCGL case, we take into account the dissipative effects. When the burst reaches a threshold height h_0, the dissipation suddenly becomes important and the burst dies out rapidly, but a burst evolves in a way similar to a singular solution of the QNLS equation before reaching h_0. The threshold height h_0 is not definite but distributed as described by a distribution density function $g(h_0)$. Therefore $P_T(h)$ is expressed by the sum of $P_B(h)$ weighted with $g(h_0)$ over various threshold heights h_0.

Note that this distribution density is expressed in terms of $G(h)$, which was introduced in § 3.2, as

$$g(h)=-\frac{dG(h)}{dh}\,. \tag{10}$$

The PDF, $P_B(h)$, of a single burst with threshold height h_0 is approximated by $P_{h_0}(h)$, which is calculated as

$$P_{h_0}(h)\propto\int_{-\infty}^{t_0}dt\int_{-\infty}^{\infty}dx\delta(h-|\psi(x,t)|) \quad (t_0 \text{ being a time s.t. } h_0=\sup_x|\psi(x,t_0)|)$$

$$=4h^{-7}\int_{-\infty}^{\infty}d\xi S(\xi)^6\theta(h_0S(\xi)-h)\,, \tag{11}$$

where

$$\theta(x)=\begin{cases}0 & \text{for } x<0\,,\\ 1 & \text{for } x>0\,,\end{cases}$$

is the Heaviside step function.

By noticing that $P_{h_0}(h)$ vanishes for $h>h_0$, and comparing Eqs. (9) and (11), we can approximate $P_{h_0}(h)$ by

$$P_{h_0}(h)\sim\theta(h_0-h)P_\infty(h)\,. \tag{12}$$

This approximation is derived since the power 6 of $S(\xi)$ in Eq. (11) indicates that only the value of $S(\xi)\sim 1$ gives contribution to the integral.

Then using Eq. (12), we have

$$P_T(h)\propto\int_0^\infty g(h_0)P_{h_0}(h)dh_0$$

$$\simeq\int_0^\infty\theta(h_0-h)g(h_0)P_\infty(h)dh_0$$

$$=P_\infty(h)\int_h^\infty g(h_0)dh_0$$

$$=P_\infty(h)G(h)\,. \tag{13}$$

Thus the PDF of $|\psi|$ for the QCGL equation can be expressed as the product of the PDF of amplitude of the singular solution of the QNLS equation and the PDF of the bursts whose maximum heights are larger than h.

As was shown, in § 3.2, $G(h)$ has a -1 power law, so that we get $P_T(h) \propto h^{-8}$. This result coincides with the numerical result.

§ 5. Concluding remarks

We examined the PDFs of ψ numerically and analytically. It is found numerically that the PDF of $|\psi|$ has an algebraic tail with power -8. This tail structure can be expressed by the product of the PDF of a single burst and the distribution of the maximum amplitudes of bursts.

Each burst blows up self-similarly like a singular solution of the QNLS equation until the dissipation starts to work in case of sufficiently weak dissipation; each bursting process is described by the non-dissipative feature. This self-similarity gives an algebraic tail with power -7 to the PDF of a single burst. The self-similarity of the bursting process is broken slightly by a logarithmic correction and a weak dependence of V on time. These effects, however, are too weak to affect the results we obtained. Thus we neglected these effects in this paper.

Bursts are, however, unavoidably depleted by arbitrary dissipation. Thus they are forced to obey some distribution. We found that this distribution, $G(h)$, takes an algebraic form asymptotically as ν increases. It is noted that $G(h)$ has a tail falling down more rapidly than algebraically at large values of h. The structure of $G(h)$ is investigated in detail numerically, but we have not yet succeeded in explanation of this structure.

These relations between statistics and structures seem to be essential for systems showing the strongly intermittent behaviors, such as the fully developed turbulence. We are now trying to apply our ideas to such systems.

Acknowledgements

The authors would like to express their cordial thanks to Professor T. Kawahara and Dr. K. Ohkitani for encouragement and improving this manuscript. One of the authors (H.I.) thanks Professor S. Kida and Professor J. Mizushima for continuous encouragement. The authors also thank Mr. S. Kishiba, Mr. K. Araki and Mr. S. Hosoda for their invaluable contribution to preparing the manuscript. This work was supported in part by a Grant-in-Aid (no. 03740200) from the Ministry of Education, Science and Culture of Japan.

References

1) U. Frisch, in *Turbulence and Predictability in Geophysical Fluid Dynamics and Climate Dynamics*, ed. M. Ghil (North-Holland, 1985), p. 71.
2) S. Kida and Y. Murakami, Fluid Dyn. Res. **4** (1989), 347.
3) M. Yamada and K. Ohkitani, Prog. Theor. Phys. **86** (1991), 759.
4) Z. -S. She, E. Jackson and S. A. Orszag, J. Sci. Comput. **3** (1988), 407.
5) R. H. Kraichnan, Phys. Rev. Lett. **65** (1990), 575.

6) Z. -S. She, Phys. Rev. Lett. **66** (1991), 600.
7) R. Benzi, L. Biferale, G. Paladin, A. Vulpiani and M. Vergassola, Phys. Rev. Lett. **67** (1991), 2299.
8) M. Brachet, D. Meiron, B. Nickel, S. Orszag and U. Frisch, J. Fluid Mech. **130** (1983), 411.
9) A. Pumir and E. D. Siggia, Phys. Fluids **30** (1987), 1606.
10) C. Sulem, P. L. Sulem and H. Frisch, J. Comp. Phys. **50** (1983), 138.
11) S. Toh and H. Iwasaki, J. Phys. Soc. Jpn. **61** (1992).
12) M. Bartuccelli, P. Constantin, C. R. Doering, J. D. Gibbon and M. Gisselfält, Physica **D44** (1990), 421.
13) I. Rasmussen and K. Rypidal, Phys. Scripta **33** (1986), 481.
K. Rypidal and I. Rasmussen, Phys. Scripta **33** (1986), 498.
14) V. E. Zakharov and V. S. Synakh, Sov. Phys. -JETP **41** (1976), 465.
15) D. Wood, Stud. Appl. Math. **71** (1984), 103.
16) B. J. LeMesurier, G. C. Papanicolaou, C. Sulem and P. L. Sulem, Physica **D32** (1988), 210.
17) M. J. Landman, G. C. Papanicolaou, C. Sulem and P. L. Sulem, Phys. Rev. **A38** (1988), 3837.
18) A. C. Newell, D. A. Rand and D. Russell, Physica **D33** (1988), 281.